Stabilization of Gold Nanoparticles by Hairpin DNA and Implications for Label-free Colorimetric Biosensors

Xun Liu[1,2], Yu Zhao[3], Yuzhe Ding[2], Jianhua Wang*[1] and Juewen Liu*[2]

1. Research Center for Analytical Sciences, Department of Chemistry, College of Sciences, Northeastern University, Shenyang, 110819, China

2. Department of Chemistry, Waterloo Institute for Nanotechnology, University of Waterloo, Waterloo, Ontario, N2L 3G1, Canada

3. State Key Lab of Metal Matrix Composites, School of Materials Science and Engineering, Shanghai Jiao Tong University, Shanghai 200240, China

Abstract

With extremely high extinction coefficients and other unique optical properties, gold nanoparticles (AuNPs) have received growing interest in developing biosensors. DNA hairpin structures are very popular probes for detection of not only DNA but also aptamer targets. This work aims to understand the effect of the structure and sequence of hairpin DNA for stabilization of AuNPs and its implications in AuNP-based label-free colorimetric biosensors. A series of hairpin DNA with various loop size from 4 to 26 bases, and sequences (random sequences, poly-A and poly-T) were tested, but there showed a similar ability to protect AuNPs from aggregation. By using hairpin DNA with a tail in the same conditions, optimal protection was achieved with a 6-base or longer tail. DNA hairpins are likely adsorbed via their tail region or with their terminal bases if no tail is present. Molecular dynamics simulations showed that the rigidity of the hairpin loop region disfavored its adsorption to AuNPs, while the flexible tail region is favored. Finally, a DNA sensing assay was conducted using different structured DNA; where hairpin DNA with a tail doubled the sensitivity compared to the tail-free hairpin.

Introduction

Oligonucleotides can adopt a wide range of folded-back loops such as hairpins, triplexes and quadruplexes.[1, 2] The formation of a hairpin plays a vital role in many biological processes, including DNA recombination, gene expression and DNA transposition.[3-5] A hairpin DNA refers to a stem-loop structure, where a few base pairs define the stem.[6, 7] The open and close of hairpins is useful for many applications from designing molecular beacons[8] to modulating the lattice parameter of DNA-assembled nanoparticle crystals.[9] In addition, most DNA aptamers and DNAzymes have a hairpin structure.[10, 11] Compared to a typical double-stranded DNA, linking the two ends to form a hairpin can drastically enhance the melting temperature.[12] DNA hairpins can also kinetically trap a system and this property has been used to develop hybridization chain reactions.[13, 14] Hairpins have been used as sensing probes and immobilized on various substrates, such as glass,[15, 16] gold,[17, 18] magnetic particles,[19] and plastics[20, 21] to construct biosensor platforms.[22-24] For some applications, one or both stems end with a tail overhang.

Gold nanoparticles (AuNPs) are at the forefront of optical biosensor development due to their high extinction coefficients, distance-dependent color, fluorescence quenching, localized surface plasmon and Raman enhancement properties.[25-28] Single-stranded DNA oligonucleotides can be adsorbed by AuNPs quickly with a high affinity, while double-stranded or well-folded DNAs are adsorbed at a slower rate. By exploiting this kinetic difference, many detection methods have been achieved using DNA aptamers and DNAzymes.[29-31] AuNPs can serve as a quencher in molecular beacons,[32, 33] and as a barcode for signal generation.[34] Nonthiolated hairpin DNA has been used to develop label-free colorimetric biosensors,[35-37] especially for hybridization chair reactions.[38-41] While some fundamental studies have been performed on AuNP/hairpin systems, such as hybridization thermodynamics and kinetics,[42] and length of tail,[1, 2, 32] a systematic understanding is still lacking.

In this work, DNA hairpins were systematically varied and the effect on the colloidal stability of AuNPs was explored. Hairpin DNAs were incubated with AuNPs, and then NaCl solutions were added for salt-introduced aggregation. It was found that hairpins with a tail could provide better stability and more sensitive colorimetric detection compared to tail-free

hairpins, which was attributed to the rigidity of the loop region using molecular dynamics simulations.

Experimental section

Preparation of AuNPs. The citrate-capped AuNPs were prepared following a previously reported method.[43] In a two-neck flask, 2 mL of 50 mM $HAuCl_4$ was added to 98 mL of water. After heating the sample to reflux, 10 mL of 38.8 mM sodium citrate was added. The solution was maintained reflux for 20 min and then cooled to room temperature. The concentration of the as-prepared AuNPs was ~13 nM based on its absorbance at 522 nm (extinction coefficient: 2.7×10^8 M^{-1} cm^{-1}).

Salt-induced AuNP aggregation. 70 μL of 6.5 nM AuNPs were incubated with a DNA (1 μM, 10 μL) for 15 min. Then, 20 μL of NaCl was added into the mixture to achieve a final concentration of NaCl of 0, 10, 20, 30, 40, 50, 60, and 70 mM, respectively. After 5 min, the UV-vis spectra were collected and the values at 522 nm and 630 nm were recorded. In addition, the AuNPs without the DNA were also measured in the similar way, except that Millipore water was used in place of DNA.

DNA sensing. The probe DNAs (including control DNA, tail-free hairpin DNA and hairpin DNA) and their corresponding target DNAs were annealed in the phosphate buffer (PB, 50 mM with 100 mM NaCl, pH 7.4) at 95℃ for 1 min and then cooled to the room temperature. For each sample, the probe DNA concentration was fixed at 10 μM, while the target DNA varied from 2 to 10 μM. The annealed DNA was diluted 10 times with Milli-Q water for further use. 70 μL of 6.5 nM AuNPs were mixed with 10 μL of the annealed DNA. After incubation for 30 min, 10 μL PB (250 mM) and 10 μL NaCl solution (0.3 M) were sequentially added to the mixture. After 5 min, the UV-vis absorbance of the AuNPs at 522 nm and 630 nm was recorded.

DNA adsorption. 10 μL of 1 μM DNA was mixed with 70 μL of 6.5 nM AuNPs and 20 μL H_2O. After 15 min, the mixture was centrifugated for 15 min at a speed of 15000 rpm. 2 μL of the supernatant was mixed with 96 μL phosphate buffer (50 mM, pH 7.4) in a 96-well plate. Then 2 μL SYBR Green I (0.5×, 0.38 μM) was added into the plate. After 5 min, the fluorescence (F_0) at 520 nm was measured by microplate reader under a 490 nm excitation.

The precipitate containing DNA-capped AuNPs was mixed with 3 μL of 1 M KCN solution and 97 μL H_2O. When the AuNPs were completely dissolved, 2 μL of the mixture and 2 μL of SYBR Green (0.5×, 0.38 μM) was added into 96 μL phosphate buffer (50 mM, pH 7.4). The fluorescence (F) was measured in the same conditions. Thus, the DNA adsorption rate (η) was calculated to be $\eta=F/(F+F_0)\times100\%$.

Molecular dynamics simulations. GROMACS version 5.1.4 was used to perform the molecular dynamics (MD) simulations.[44] The simulation supercells were cuboid boxes of 70 × 90 × 70 $Å^3$, which consist of saline solution, an AuNP and a hairpin RNA (RCSB ID: 2LDL). A 6-base tail was constructed by deleting 6 nucleotides in one end and the used sequence was 5′-GGAUCCAUUCGAUUAGUGAAC. Amber14SB and TIP3P were used to model DNA/ions and water molecules, respectively.[45, 46] The electrostatic interactions were evaluated by using a particle-mesh Ewald (PME) summation, with a real space cutoff of 14 Å.[47] The Lennard-Jones (L-J) nonbonded interactions were smoothly tapered to zero when the two atoms were close to 14 Å. Three-dimensional periodic boundary conditions were applied in the simulations, and all the simulations were performed with a time step of 2 fs. The temperature was maintained at 300 K under the NVT ensemble for 100 ns via the V-rescale thermostat.

Results and Discussion

Using salt to probe DNA hairpin adsorption. A classic hairpin with a simple stem-loop structure (Figure 1A) might interact with AuNPs via the loop region, since the stem is in the duplex state and the bases are shielded. Nevertheless, the stem region might also interact with the AuNPs via the terminal bases, and such interactions were reported for DNA adsorption on graphene and gold.[48-50] For either interaction mode, DNA adsorption to gold surface via strong base coordination.[26, 51] For many applications such as hybridization chain reactions,[14] hairpins with a tail are used (Figure 1B), and the hairpins can interact with AuNPs via both the loop region and the tail. DNA plays an important role in increasing the colloidal stability of AuNPs (Figure 1C).[52] In this work, both simple hairpins and hairpins with a tail were studied. The length and sequence of the loop region and the tail were systematically varied, and their effects were evaluated by the colloidal stability of AuNPs.

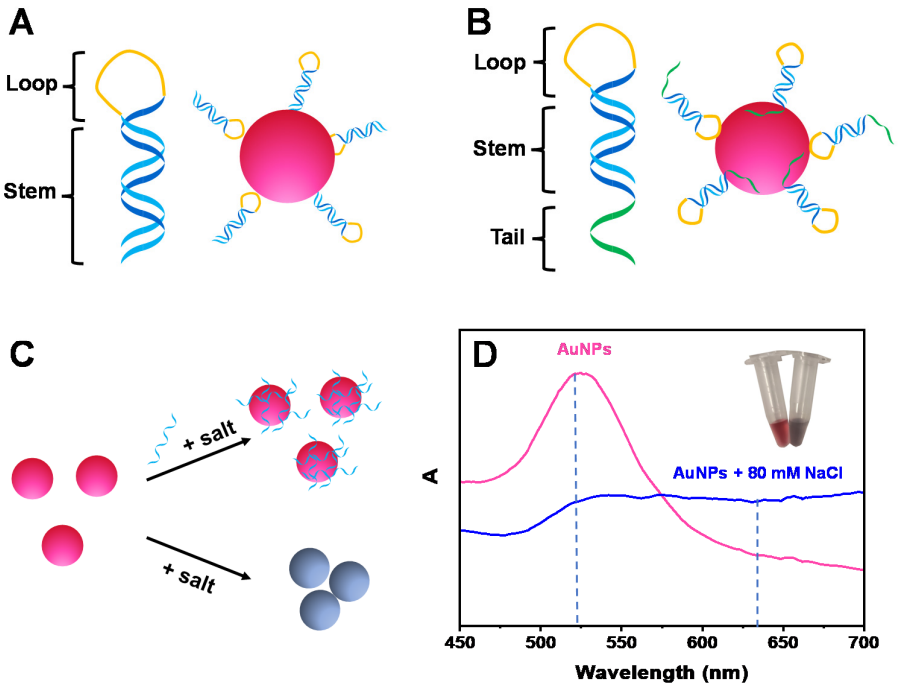


Figure 1. Schematic diagram of (A) a classic hairpin DNA, (B) a hairpin DNA with a tail and their possible ways of adsorption to AuNPs. (C) Schematic diagram of DNA protection of AuNPs from salt-induced aggregation. (D) UV-vis spectra and photographs of AuNPs without and with 80 mM NaCl.

AuNPs of 13 nm diameter were synthesized by citrate reduction, and the surface was capped with citrate ligands to provide charge stabilization.[51, 53] Their wine-like red color was due to the surface plasmon peak at 522 nm. Addition of salt caused aggregation of the AuNPs and a color change from red to purple. In this work, NaCl was used as a probe to test the colloidal stability of AuNPs. From the UV-vis spectra (Figure 1D), the absorption peak of AuNPs at 522 nm decreased obviously, while absorbance in the longer wavelength region increased with the addition of 80 mM NaCl. Therefore, the stability was evaluated by measuring absorption ratio of 630 nm over 522 nm. Well dispersed AuNPs have a low ratio of 0.2, whereas aggregated AuNPs have a high ratio close to 1.

The hairpin tail is more important for adsorption than the loop. A hairpin studied in this work has three domains: a loop, a stem and an optional tail. Since single-strained DNA (ssDNA) is more easily absorbed by AuNPs compared to double-strained DNA (dsDNA), we focused

on the loop and tail domains in this work. A series of hairpin DNAs were first designed with different base counts in the loop domain from 4 to 26, and the length of the stem was varied accordingly to retain the same total length of 48-mer (Figure 2A). The shortest stem had 8 base pairs, which is sufficiently stable for support the hairpin structure. The bases in the loop are random, and each hairpin contained a 6-nucleotide tail with a random sequence. These hairpins were respectively incubated with the AuNPs for 15 min and then NaCl of various concentrations were added. After 5 min, the absorbance was measured at 522 nm (A_{522}) and 630 nm (A_{630}) and the A_{630}/A_{522} ratio was calculated. Without the protection of a hairpin DNA (Figure 2B, black line), the AuNPs remained stable with 10 mM NaCl, although the AuNPs nearly fully aggregated in the presence of 40 mM NaCl. Adding even more NaCl did not further change the A_{630}/A_{522} ratio.

All the hairpins protected the AuNPs. With 20 to 40 mM NaCl, an obvious protection effect was observed compared to the DNA-free AuNPs. The size of the loop domain had little effect on AuNPs stability. This observation suggested other factors dominated the interaction between hairpin DNA and AuNPs, and most likely the adsorption was achieved via the tail region.

To further investigate the protection ability, two hairpin DNAs were designed with all adenine (Loop-PolyA) or thymine (Loop-PolyT) in loop (Figure 2C) and they were compared with two 15-mer linear DNA: A_{15} and T_{15}. The four types of DNA differed significantly in their protection ability (Figure 2D). For the two linear DNAs, A_{15} had a superior stabilization effect compared with T_{15}, which was consistent with the literature report that adenine can adsorb on AuNPs more strongly compared to thymine.[51, 54] However, little difference was observed for the Loop-PolyA and Loop-PolyT, which confirmed that the loop domain was not the main factor.

In addition, although Loop-PolyA (22A in its loop domain) had more adenine counts than A_{15}, Loop-PolyA-capped AuNPs had a poorer salt tolerance. In comparison to T_{15}, Loop-PolyT could more efficiently protect the AuNPs from salt-induced aggregation. These results also supported the importance of the tail adsorption. A linear DNA is more flexible allowing for better adsorption to AuNP, whereas the steric hindrance of the hairpin structure might impair the loop-mediated adsorption.

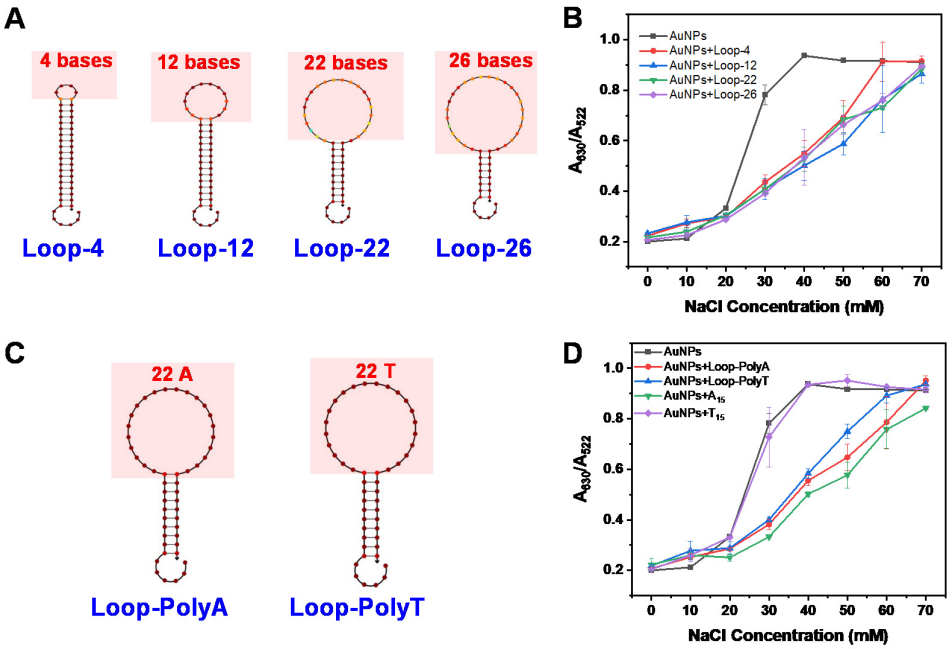


Figure 2. (A) Hairpin DNA with different bases in the loop domain. (B) The A_{630}/A_{522} ratios of the citrate-capped AuNPs in the presence of hairpin DNA with different loop lengths at 5 min after adding different concentrations of NaCl. (C) Hairpin DNA with A_{22} or T_{22} in the loop domain. (D) The A_{630}/A_{522} ratios of the citrate-capped AuNPs in the presence hairpin DNA with A_{22} or T_{22} in the loop at 5 min after adding different concentrations of NaCl.

Tail-free hairpins. To further confirm the role of the tail domain, tail-free hairpins were then used for the experiment (Figure 3A). The four hairpin DNAs had a moderate protection effect when the NaCl concentration was below 40 mM (Figure 3B), whereas beyond 40 mM, the protection provided by the hairpin DNA was minimal. Although the four hairpin DNAs had different loop sizes, they had similar AuNPs protective properties. This observation also supported the conclusion that the loop region was not important for the protection of AuNPs. Therefore, changing the length and composition of the loop would not significantly change the protection ability of hairpin DNA to AuNPs.

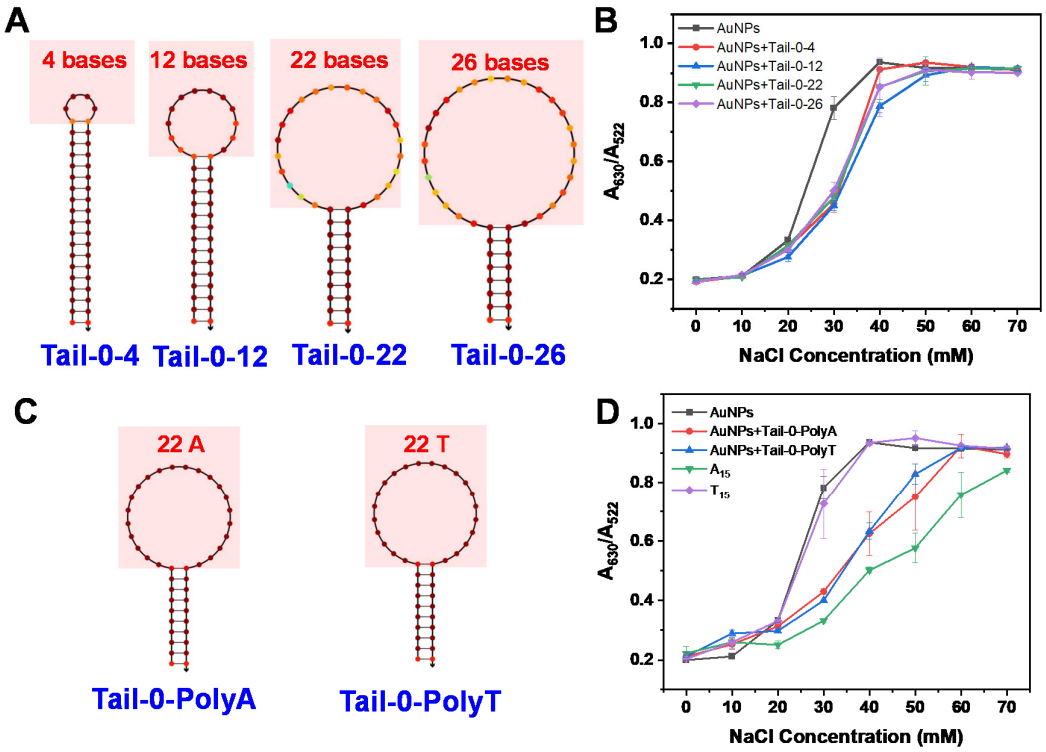


Figure 3. (A) The tail-free DNA with different bases in the loop domain. (B) The A_{630}/A_{522} ratios of the citrate-capped AuNPs in the presence of the tail-free hairpin DNA with different loop sizes at 5 min after adding different concentrations of NaCl. (C) The tail-free hairpin DNA with A_{22} or T_{22} in the loop domain. (D) The A_{630}/A_{522} ratios of the citrate-capped AuNPs in the presence the tail-free hairpin DNAs with A_{22} or T_{22} in the loop at 5 min after adding different concentrations of NaCl.

The two tail-free hairpins were tested with all the bases of loop domain replaced with A or T (Tail-0-PolyA and Tail-0-PolyT, Figure 3C). These two hairpin DNAs were compared with A_{15} and T_{15} for their ability to protect the AuNPs (Figure 3D). The A_{15}-capped AuNPs had the highest colloidal stability among them, while the T_{15}-capped AuNPs had the lowest stability. Although the hairpin DNAs did not contain a tail, they had the ability to prevent AuNPs from salt-introduced aggregation. This protective ability had little to do with the size or the sequence of the loop. Thus, we reason that the tail-free hairpin DNAs were adsorbed via the terminal bases.

Effect of the tail domain. After confirming the importance of the tail domain, four hairpin

DNAs were designed with different base numbers in the tail (Figure 4A). As shown in Figure 4B, the hairpins with 9 or 6 bases in tail domain best protected the AuNPs and their protection effect was similar. However, when the tail shrank to 3 bases, the protective ability was significantly reduced, similar to the tail-free hairpin. Therefore, a 6-base tail is sufficient to achieve good protection.

To explain the different protective ability among various hairpin and linear DNA, the DNA density was measured in the same conditions (Figure 4C). Due to a high affinity, A_{15} had the highest adsorption efficiency of 83%. However, the hairpin DNA density on the surface of AuNPs decreased significantly. The adsorbed DNA was only 51% and 44% for Tail-9 and Tail-6, respectively. For Tail-3 and Tail-0, the DNA adsorption was less than 20%. This can also explain why Tail-3 and Tail-0 provided less protective ability than Tail-9 and Tail-6 for the AuNPs.[55, 56]

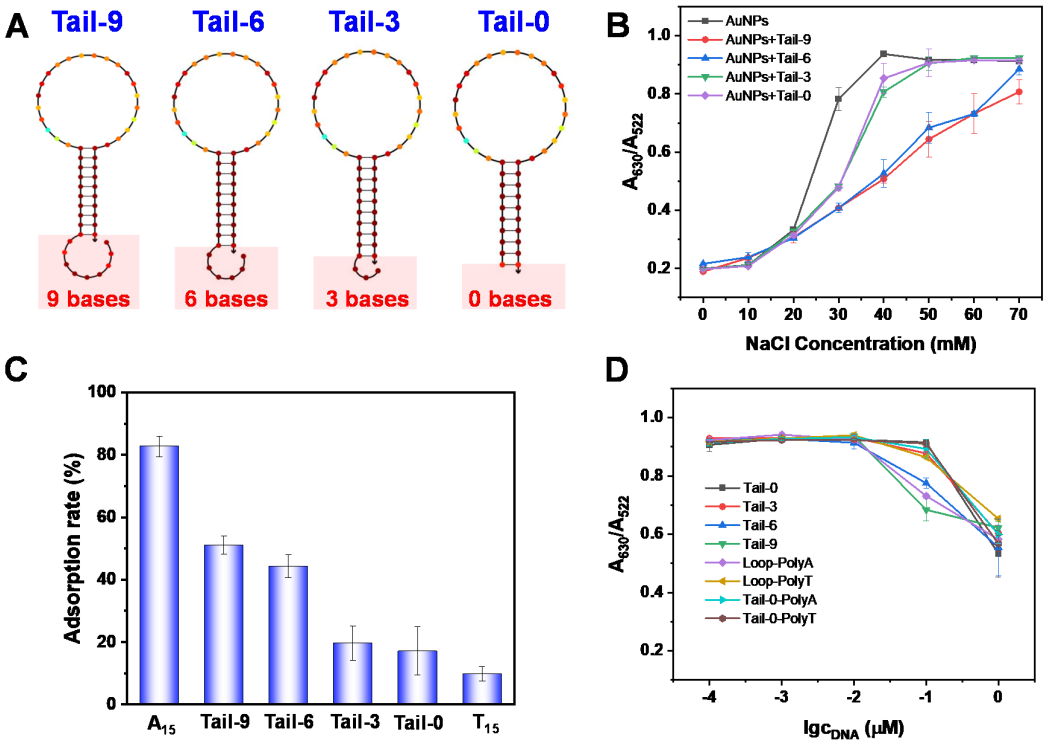


Figure 4. (A) Hairpin DNA with different bases in the tail domain. (B) The A_{630}/A_{522} ratios of the citrate-capped AuNPs in the presence of hairpin DNA with different tail length at 5 min after adding different concentrations of NaCl. (C) The percentage of adsorbed DNA on the surface of AuNPs, in which 0.1 μM DNA and 4.5 nM AuNPs were mixed in phosphate buffer (50 mM, pH 7.4). (D) Effect of hairpin DNA concentration on the color of the AuNPs

quantified by the absorbance ratio.

The above studied used the same final DNA concentration of 0.1 μM. The effect of hairpin DNA concentration on the protection was also studied (Figure 4C). When the DNA concentration was very low (10 nM or lower), little protection effect was observed. Since 6.5 nM AuNPs was used, each AuNP had less than 2 DNA strands with 10 nM DNA, which can explain the low stability. However, when the DNA concentration reached 1 μM, the protection effect was similar, disallowing us to distinguish the protective ability of different hairpin DNA. Therefore, we used 0.1 μM DNA for most experiments.

Molecular dynamics simulations. To further understand the more efficient adsorption of the tail instead of the loop of hairpins, we performed MD simulations. We took the structure of a hairpin RNA (RCSB ID: 2LDL) and deleted 6 bases to create a 6-nucleotide tail and then studied its adsorption by an AuNP. The root-mean-square-deviation (RMSD) and adsorption energy (Figure S1) showed the hairpin adsorbed on the AuNP after 1 ns. Further, the adsorption conformations in Figure 5A show that, the tail preferentially adsorbs to the gold surface and gradually stabilizes, while the loop region is not easy to adsorb for its rigid secondary structure. Most of the loops in DNA hairpins tend to form various secondary structures. Due to a steric hindrance effect, both the bases and the phosphate backbones of loops are less structurally mobile and have fewer binding sites for gold surface than the flexible tail.

Taken together, the size and sequence of the loop domain did not have much effect on the stability of the AuNPs, while more bases in the tail domain are favorable. Based on our results, we ranked the stabilization ability of hairpin DNA and ssDNA for AuNPs in Figure 5B.

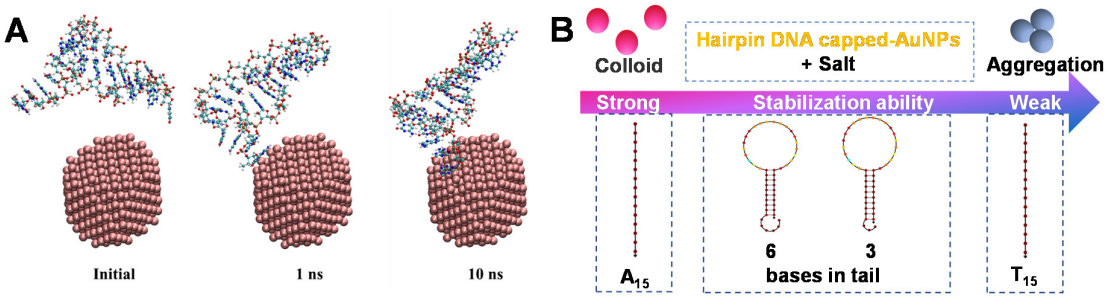


Figure 5. (A) The adsorption conformations of a hairpin with a 6-nucleotide tail during the MD simulations. (B) Comparison of stability of AuNPs in the presence of different linear and hairpin DNA.

Application for DNA detection. After observing the relative protection effect of different hairpin structures, we then used this understanding in label-free colorimetric detection. Three DNA probes were compared: a random coil (probe 1), a simple hairpin (probe 2) and a tail containing hairpin (probe 3). The complementary target was added to the probe DNAs to form dsDNA. For probe 3, two types of target DNAs were added, and one of them resulted in a tail in the final duplex product. The hairpin probe samples with different concentrations of target DNA were then mixed with the AuNPs and salt was added. The sensing principle is shown in Figure 6A. Single-stranded DNA (ssDNA) can bind and stabilize AuNPs, while double-stranded DNA (dsDNA) cannot. After adding NaCl, the absorbance ratio was plotted to construct the standard curves (Figure 6B).

For probe 1 with a random coil structure, this sensor had a low background because the DNA adsorbed well on the surface of AuNPs and stabilized the colloid. In this case, a superior sensitivity was obtained (Figure 6B, black line, $A_{630}/A_{522}=0.0036c_{DNA}+0.5688$, $R^2=0.997$). However, for the hairpin DNA without a tail (probe 2), it did not efficiently stabilize the AuNPs resulting in a high background signal, which greatly reduced the sensitivity (red line, $A_{630}/A_{522}=0.0007c_{DNA}+0.8991$, $R^2=0.979$). When the assay was conducted using a hairpin DNA with a tail (probe 3) and a fully complementary DNA as a target (target 3), a better sensitivity was observed (blue line, $A_{630}/A_{522}=0.0014c_{DNA}+0.6836$, $R^2=0.956$). Finally, for mixing probe 3 with the partially complimentary DNA target (target 4), a fraction of ssDNA sequence remained after hybridization, which provided strong protection ability to the AuNPs. Therefore, a high target DNA concentration did not cause a significant signal change (green line, $A_{630}/A_{522}=0.0006c_{DNA}+0.7112$, $R^2=0.956$). Since the slopes of these calibration curves are defined as the sensitivity of the sensors, we compared the slopes or sensitivity in Figure 6C. It can be concluded that having a hairpin probe would decrease the sensitivity. Among the different hairpins, having a tail in the hairpin DNA probe would enhance sensitivity of sensing assay, while having a tail in the duplex product would decrease the sensitivity.

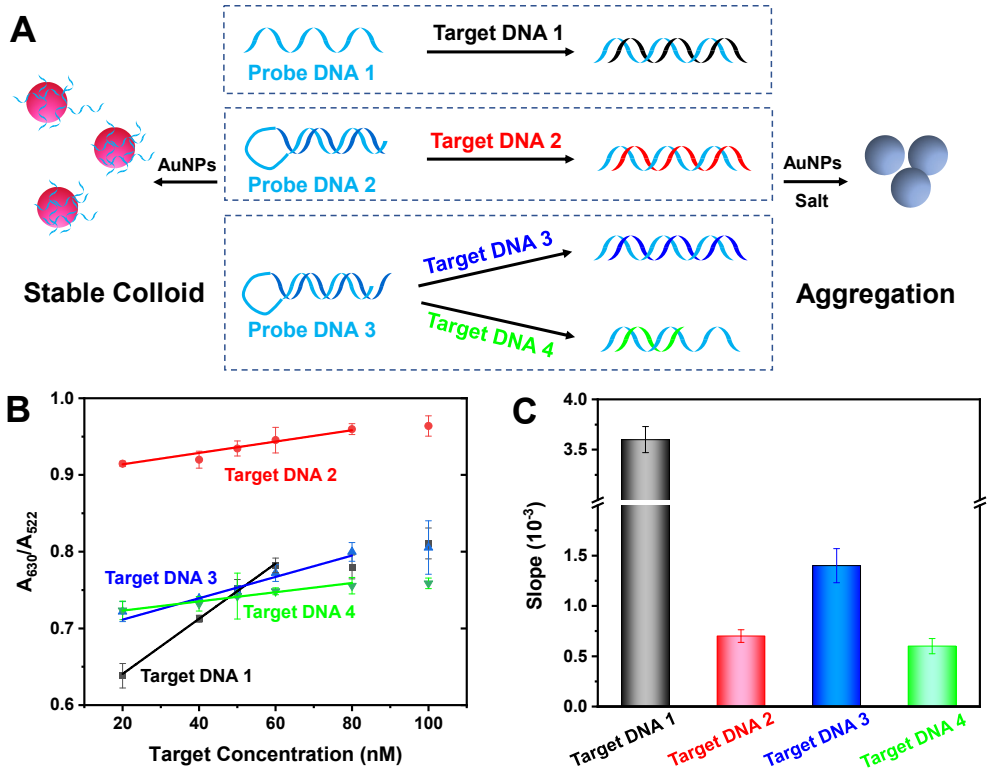


Figure 6. (A) Scheme for the three types of DNA probes for label-free colorimetric detection of DNA. For probe 3, its hybridization to target 4 resulted in a duplex with an overhang. (B) Calibration curves for the detection showing dependence of A_{630}/A_{522} upon reacting with target DNA of different concentrations. (C) The comparison of the sensitivity of the different sensors, and the sensitivity is defined as the slopes of the calibration curves.

Conclusions

In this work, hairpin DNAs were systematically studied with different structures for their ability to protect the colloidal stability of AuNPs. According to the change of A_{630}/A_{522} in the presence of different NaCl concentrations, the tail domain in hairpin DNA played a more important in stabilizing AuNPs than the loop domain. For the tail-free hairpins, they were likely adsorbed via the terminal bases in the stem region. Based on molecular dynamics simulation, the rigidity of the hairpin loop region could be the reason for its disfavored adsorption. Finally, three DNA probes were explored which consisted of a random coil, a simple tail-free hairpin and a tail-containing hairpin in label-free colorimetric sensing. Among them, the random coil had the

highest sensitivity. The hairpin with a tail provided better sensitivity in comparison to the tail-free hairpin. Therefore, the adsorption of hairpin DNA to AuNPs can be fine-tuned by adjusting the structure of hairpin DNA, which is important for improving the sensitivity of hairpin DNA based sensors.

Supporting Information

Chemical and materials; instrumentation; the DNA sequences used in this work (Table S1); and molecular dynamics simulation data (PDF).

Author Information

Corresponding Authors

Jianhua Wang: Department of Chemistry, College of Sciences, Northeastern University, Shenyang 110819, China;

Email: jianhuajrz@mail.neu.edu.cn

Juewen Liu: Department of Chemistry, Waterloo Institute for Nanotechnology, University of Waterloo, Waterloo, Ontario N2L 3G1, Canada;

Email: liujw@uwaterloo.ca

Acknowledgements

Funding for this work was from the Natural Sciences and Engineering Research Council of Canada (NSERC). X. Liu received a China Scholarship Council Scholarship to visit the University of Waterloo.

Notes

The authors declare no competing financial interest.

References

1. Blose, J. M.; Lloyd, K. P.; Bevilacqua, P. C., Portability of the GN(R)A Hairpin Loop Motif between RNA and DNA. *Biochemistry* **2009,** *48* (37), 8787-8794.

2. Antao, V. P.; Tinoco, I., Jr, Thermodynamic parameters for loop formation in RNA and DNA hairpin tetraloops. *Nucleic Acids Res.* **1992,** *20* (4), 819-824.

3. Roth, D. B.; Menetski, J. P.; Nakajima, P. B.; Bosma, M. J.; Gellert, M., V(D)J recombination: Broken DNA molecules with covalently sealed (hairpin) coding ends in scid mouse thymocytes. *Cell* **1992,** *70* (6), 983-991.

4. Bhasin, A.; Goryshin, I. Y.; Reznikoff, W. S., Hairpin formation in Tn5 transposition. *J. Biol. Chem.* **1999,** *274* (52), 37021-37029.

5. Kennedy, A. K.; Guhathakurta, A.; Kleckner, N.; Haniford, D. B., Tn10 Transposition via a DNA Hairpin Intermediate. *Cell* **1998,** *95* (1), 125-134.

6. Tsourkas, A.; Behlke, M. A.; Rose, S. D.; Bao, G., Hybridization kinetics and thermodynamics of molecular beacons. *Nucleic Acids Res.* **2003,** *31* (4), 1319-1330.

7. Huang, J.; Wu, J.; Li, Z., Biosensing using hairpin DNA probes. *Rev. Anal. Chem.* **2015,** *34* (1-2), 1-27.

8. Wang, K.; Tang, Z.; Yang, C. J.; Kim, Y.; Fang, X.; Li, W.; Wu, Y.; Medley, C. D.; Cao, Z.; Li, J.; Colon, P.; Lin, H.; Tan, W., Molecular Engineering of DNA: Molecular Beacons. *Angew. Chem. Int. Ed.* **2009,** *48* (5), 856-870.

9. Laramy, C. R.; O'Brien, M. N.; Mirkin, C. A., Crystal engineering with DNA. *Nat. Rev. Mater.* **2019,** *4* (3), 201-224.

10. Zhou, W.; Saran, R.; Liu, J., Metal Sensing by DNA. *Chem. Rev.* **2017,** *117* (12), 8272-8325.

11. Yu, H.; Alkhamis, O.; Canoura, J.; Liu, Y.; Xiao, Y., Advances and Challenges in Small-Molecule DNA Aptamer Isolation, Characterization, and Sensor Development. *Angew. Chem. Int. Ed.* **2021,** *60* (31), 16800-16823.

12. Zhang, H.; Li, F.; Dever, B.; Wang, C.; Li, X.-F.; Le, X. C., Assembling DNA through Affinity Binding to Achieve Ultrasensitive Protein Detection. *Angew. Chem. Int. Ed.* **2013,** *52* (41), 10698-10705.

13. Kachwala, M. J.; Smith, C. W.; Nandu, N.; Yigit, M. V., Reprogrammable Gel Electrophoresis Detection Assay Using CRISPR-Cas12a and Hybridization Chain Reaction. *Anal. Chem.* **2021,** *93* (4), 1934-1938.

14. Chen, Y.; Gong, X.; Gao, Y.; Shang, Y.; Shang, J.; Yu, S.; Li, R.; He, S.; Liu, X.; Wang, F.,

Bioorthogonal regulation of DNA circuits for smart intracellular microRNA imaging. *Chem. Sci.* **2021,** *12* (47), 15710-15718.

15. Guo, Q.; Bai, Z.; Liu, Y.; Sun, Q., A molecular beacon microarray based on a quantum dot label for detecting single nucleotide polymorphisms. *Biosens. Bioelectron.* **2016,** *77*, 107-110.

16. Yang, X.; Liu, Q.; Wen, D.; Gao, M.; Zhang, D.; Jin, Q.; Kong, J.; Zhang, J., Ultrasensitive fluorescence detection of sequence-specific DNA via labeling hairpin DNA probes for fluorescein o-acrylate polymers. *Anal. Chim. Acta* **2019,** *1088*, 144-149.

17. Zhao, J.; He, C.; Wu, W.; Yang, H.; Dong, J.; Wen, L.; Hu, Z.; Yang, M.; Hou, C.; Huo, D., MXene-MoS_2 heterostructure collaborated with catalyzed hairpin assembly for label-free electrochemical detection of microRNA-21. *Talanta* **2022,** *237*, 122927.

18. Zou, L.; Li, X.; Lai, Y., Colorimetric aptasensor for sensitive detection of kanamycin based on target-triggered catalytic hairpin assembly amplification and DNA-gold nanoparticle probes. *Microchem. J.* **2021,** *162*, 105858.

19. Oishi, M.; Juji, S., Acceleration of DNA Hybridization Chain Reactions on 3D Nanointerfaces of Magnetic Particles and Their Direct Application in the Enzyme-Free Amplified Detection of microRNA. *ACS Appl. Mater. Interfaces* **2021,** *13* (30), 35533-35544.

20. Shi, X.; Wen, J.; Li, Y.; Zheng, Y.; Zhou, J.; Li, X.; Yu, H.-Z., DNA Molecular Beacon-Based Plastic Biochip: A Versatile and Sensitive Scanometric Detection Platform. *ACS Appl. Mater. Interfaces* **2014,** *6* (24), 21788-21797.

21. Zhang, L.; Wong, J. X. H.; Li, X.; Li, Y.; Yi, H.-Z., Detection and Quantitation of Heavy Metal Ions on Bona Fide DVDs Using DNA Molecular Beacon Probes. *Anal. Chem.* **2015,** *87* (10), 5062-5067.

22. Shi, X.; Gao, X.; Zhang, L.; Li, Y.; Fan, L.; Yu, H.-Z., Binary DNA hairpin-based colorimetric biochip for simultaneous detection of Pb^{2+} and Hg^{2+} in real-world samples. *Analyst* **2015,** *140* (8), 2608-2612.

23. Baker, B. R.; Lai, R. Y.; Wood, M. S.; Doctor, E. H.; Heeger, A. J.; Plaxco, K. W., An electronic, aptamer-based small-molecule sensor for the rapid, label-free detection of cocaine in adulterated samples and biological fluids. *J. Am. Chem. Soc.* **2006,** *128* (10), 3138-3139.

24. Pan, W.; Zhang, T.; Yang, H.; Diao, W.; Li, N.; Tang, B., Multiplexed Detection and Imaging of Intracellular mRNAs Using a Four-Color Nanoprobe. *Anal. Chem.* **2013,** *85* (21),

10581-10588.

25. Song, S.; Qin, Y.; He, Y.; Huang, Q.; Fan, C.; Chen, H.-Y., Functional nanoprobes for ultrasensitive detection of biomolecules. *Chem. Soc. Rev.* **2010,** *39* (11), 4234-4243.

26. Liu, B.; Liu, J., Interface-Driven Hybrid Materials Based on DNA-Functionalized Gold Nanoparticles. *Matter* **2019,** *1* (4), 825-847.

27. Wang, H.; Yang, R.; Yang, L.; Tan, W., Nucleic Acid Conjugated Nanomaterials for Enhanced Molecular Recognition. *ACS Nano* **2009,** *3* (9), 2451-2460.

28. Qiu, C.; Cheng, Z.; Lv, C.; Wang, R.; Yu, F., Development of bioorthogonal SERS imaging probe in biological and biomedical applications. *Chin. Chem. Lett.* **2021,** *32* (8), 2369-2379.

29. Zheng, Y.; Wang, Y.; Yang, X., Aptamer-based colorimetric biosensing of dopamine using unmodified gold nanoparticles. *Sens. Actuators B Chem* **2011,** *156* (1), 95-99.

30. Liu, X.; He, F.; Zhang, F.; Zhang, Z.; Huang, Z.; Liu, J., Dopamine and Melamine Binding to Gold Nanoparticles Dominates Their Aptamer-Based Label-Free Colorimetric Sensing. *Anal. Chem.* **2020,** *92* (13), 9370-9378.

31. Wang, Z.; Lee, J. H.; Lu, Y., Label-free colorimetric detection of lead ions with a nanomolar detection limit and tunable dynamic range by using gold nanoparticles and DNAzyme. *Adv. Mater.* **2008,** *20* (17), 3263-3267.

32. Jayagopal, A.; Halfpenny, K. C.; Perez, J. W.; Wright, D. W., Hairpin DNA-Functionalized Gold Colloids for the Imaging of mRNA in Live Cells. *J. Am. Chem. Soc.* **2010,** *132* (28), 9789-9796.

33. Wei, G.; Yu, J.; Wang, J.; Gu, P.; Birch, D. J. S.; Chen, Y., Hairpin DNA-functionalized gold nanorods for mRNA detection in homogenous solution. *J. Biomed. Optics* **2016,** *21* (9), 097001.

34. Cui, H.-F.; Xu, T.-B.; Sun, Y.-L.; Zhou, A.-W.; Cui, Y.-H.; Liu, W.; Luong, J. H. T., Hairpin DNA as a Biobarcode Modified on Gold Nanoparticles for Electrochemical DNA Detection. *Anal. Chem.* **2015,** *87* (2), 1358-1365.

35. He, H.; Dai, J.; Duan, Z.; Zheng, B.; Meng, Y.; Guo, Y.; Xiao, D., Unusual sequence length dependent gold nanoparticles aggregation of the ssDNA sticky end and its application for enzyme-free and signal amplified colorimetric DNA detection. *Sci. Rep.* **2016,** *6*, 30878.

36. Chen, S.; Zong, X.; Zheng, J.; Zhang, J.; Zhou, M.; Chen, Q.; Man, C.; Jiang, Y., A

Colorimetric Strategy Based on Aptamer-Catalyzed Hairpin Assembly for the On-Site Detection of Salmonella typhimurium in Milk. *Foods* **2021,** *10* (11), 2539.

37. Huang, Z.; Chen, J.; Luo, Z.; Wang, X.; Duan, Y., Label-Free and Enzyme-Free Colorimetric Detection of Pb^{2+} Based on RNA Cleavage and Annealing-Accelerated Hybridization Chain Reaction. *Anal. Chem.* **2019,** *91* (7), 4806-4813.

38. Yuan, D.; Fang, X.; Liu, Y.; Kong, J.; Chen, Q., A hybridization chain reaction coupled with gold nanoparticles for allergen gene detection in peanut, soybean and sesame DNAs. *Analyst* **2019,** *144* (12), 3886-3891.

39. Miao, X.; Ning, X.; Li, Z.; Cheng, Z., Sensitive detection of miRNA by using hybridization chain reaction coupled with positively charged gold nanoparticles. *Sci. Rep.* **2016,** *6*, 32358.

40. Liu, P.; Yang, X.; Sun, S.; Wang, Q.; Wang, K.; Huang, J.; Liu, J.; He, L., Enzyme-Free Colorimetric Detection of DNA by Using Gold Nanoparticles and Hybridization Chain Reaction Amplification. *Anal. Chem.* **2013,** *85* (16), 7689-7695.

41. Wang, Q.; Yang, X.; Yang, X.; Liu, P.; Wang, K.; Huang, J.; Liu, J.; Song, C.; Wang, J., Colorimetric detection of mercury ion based on unmodified gold nanoparticles and target-triggered hybridization chain reaction amplification. *Spectrochim. Acta A* **2015,** *136*, 283-287.

42. Chen, C.; Wang, W.; Ge, J.; Zhao, X. S., Kinetics and thermodynamics of DNA hybridization on gold nanoparticles. *Nucleic Acids Res.* **2009,** *37* (11), 3756-3765.

43. Liu, J.; Lu, Y., Preparation of aptamer-linked gold nanoparticle purple aggregates for colorimetric sensing of analytes. *Nat. Protoc.* **2006,** *1* (1), 246-252.

44. Hess, B.; Kutzner, C.; van der Spoel, D.; Lindahl, E., GROMACS 4: Algorithms for highly efficient, load-balanced, and scalable molecular simulation. *J. Chem. Theory Comput.* **2008,** *4* (3), 435-447.

45. Maier, J. A.; Martinez, C.; Kasavajhala, K.; Wickstrom, L.; Hauser, K. E.; Simmerling, C. Ff14sb: Improving the Accuracy of Protein Side Chain and Backbone Parameters from Ff99sb. *J. Chem. Theory Comput.* **2015**, *11* (8), 3696-3713.

46. Jorgensen, W. L.; Chandrasekhar, J.; Madura, J. D.; Impey, R. W.; Klein, M. L., Comparison of simple potential functions for simulating liquid water. *J. Chem. Phys.* **1983,** *79* (2), 926-935.

47. Darden, T.; York, D.; Pedersen, L., Particle mesh Ewald: An Nlog(N) method for Ewald

sums in large systems. *J. Chem. Phys.* **1993,** *98* (12), 10089-10092.

48. Zhao, X., Self-Assembly of DNA Segments on Graphene and Carbon Nanotube Arrays in Aqueous Solution: A Molecular Simulation Study. *J. Phys. Chem. C* **2011,** *115* (14), 6181-6189.

49. Farkhari, N.; Abbasian, S.; Moshaii, A.; Nikkhah, M., Mechanism of adsorption of single and double stranded DNA on gold and silver nanoparticles: Investigating some important parameters in bio-sensing applications. *Colloids Surf. B* **2016,** *148*, 657-664.

50. Huang, Z.; Liu, B.; Liu, J., Parallel Polyadenine Duplex Formation at Low pH Facilitates DNA Conjugation onto Gold Nanoparticles. *Langmuir* **2016,** *32* (45), 11986-11992.

51. Kimura-Suda, H.; Petrovykh, D. Y.; Tarlov, M. J.; Whitman, L. J., Base-dependent competitive adsorption of single-stranded DNA on gold. *J. Am. Chem. Soc.* **2003,** *125* (30), 9014-9015.

52. Li, H. X.; Rothberg, L. J., Label-free colorimetric detection of specific sequences in genomic DNA amplified by the polymerase chain reaction. *J. Am. Chem. Soc.* **2004,** *126* (35), 10958-10961.

53. Park, J.-W.; Shumaker-Parry, J. S., Structural Study of Citrate Layers on Gold Nanoparticles: Role of Intermolecular Interactions in Stabilizing Nanoparticles. *J. Am. Chem. Soc.* **2014,** *136* (5), 1907-1921.

54. Liu, B.; Wu, P.; Huang, Z.; Ma, L.; Liu, J., Bromide as a Robust Backfiller on Gold for Precise Control of DNA Conformation and High Stability of Spherical Nucleic Acids. *J. Am. Chem. Soc.* **2018,** *140* (13), 4499-4502.

55. Pei, H.; Li, F.; Wan, Y.; Wei, M.; Liu, H.; Su, Y.; Chen, N.; Huang, Q.; Fan, C., Designed Diblock Oligonucleotide for the Synthesis of Spatially Isolated and Highly Hybridizable Functionalization of DNA-Gold Nanoparticle Nanoconjugates. *J. Am. Chem. Soc.* **2012,** *134* (29), 11876-11879.

56. Zhang, X.; Liu, B.; Dave, N.; Servos, M. R.; Liu, J., Instantaneous Attachment of an Ultrahigh Density of Nonthiolated DNA to Gold Nanoparticles and Its Applications. *Langmuir* **2012,** *28* (49), 17053-17060.

For TOC graphics only

